Sci. Rep. Kanazawa Univ.
Vol. 43, No. 2, pp. 1-11
December 1998

Electron microprobe element image of zoned chromian spinel with hydrous mineral inclusions in a chromitite from Elistratova ophiolite, Far East Russia

Tatsuki TSUJIMORI*, Daichi SAITO*, Akira ISHIWATARI*, Sumio MIYASHITA**
and Sergei D. SOKOLOV†

*) *Department of Earth Science, Faculty of Science, Kakuma, Kanazawa University, Kanazawa 920-1192, Japan*
**) *Department of Geology, Faculty of Science, Niigata University, Ikarashi, Niigata 950-2181, Japan*
†) *Geological Institute, Russian Academy of Sciences, Pyzhevsky 7, Moscow 109017, Russia*

Abstract: Cr, Si, Al and Fe distribution in some zoned chromian spinels in a chromitite from Elistratova ophiolite, Far East Russia, is mapped by electron-probe microanalyzer. A large number of mineral inclusions such as hornblende, Na-phlogopite, K-phlogopite and orthopyroxene occur restricted only in a lighter-colored core or in some cases in a "ring" containing significantly higher Al and lower Fe. The compositional anomaly thoroughly follows the distribution of inclusions, and is recognized only in the inclusion-bearing "core" or "ring" of a chromian spinel grain. The Elistratova chromitite may be a product of melt/mantle interaction and related melt mixing. The symmetric compositional zoning of chromian spinel may be related to incomplete reaction with melt of changing composition. The Fe^{3+} zoning at inclusion-bearing part may reflect change in melt composition and oxygen fugacity during chromian spinel growth. The hydrous melt to produce hydrous mineral inclusions may contain some reducing volatile components such as H_2 and CH_4.

1. Introduction

Solid phase inclusions within compositionally zoned minerals are commonly observed in both metamorphic and igneous minerals, such as garnet, pyroxenes and plagioclase. The inclusion species and chemical composition of host minerals provide various information to reveal petrogenetic processes, because they are entrapped during growth of the host mineral. Remarkably zoned chromian spinel with hydrous mineral inclusions was found in a chromitite block in the Elistratova ophiolite, Far East Russia. Hydrous mineral inclusion in chromian spinel is a key to understand chromitite genesis at upper mantle and to consider tectonic setting of the Elistratova ophiolite. In addition to these interests, the zoned chromian spinel in chromitite, extremely rare in itself, serves evidence for the role

of fluid and melt composition in the formation of chromitite. In this paper, we present electron microprobe element image of the zoned chromian spinel in chromitite from Elistratova ophiolite.

2. Geologic outline

The eastern coastal terrain of Taigonos Peninsula faces the western coast of Kamchatka over Penzhina Bay. The terrain is composed of sediments and ophiolites of early Paleozoic to Cretaceous ages, comprising the southernmost part of the accretionary complexes of the Koryak Mountains. In August 1997, we made a joint field research on the Elistratova ophiolite (6×20 km) on the eastern coast of Taigonos Peninsula (Ishiwatari et al., 1998; Saito et al., in press).

The Elistratova ophiolite is exposed in the 6×20 km area (N 61°35', E 163°), and includes all members such as residual mantle peridotite, cumulate ultramafic rocks, gabbro, sheeted dikes, and basaltic rocks (Fig. 1) (Belyi and Akinin, 1985 ; Saito et al., in press). The ophiolite area is divided into three zones trending NE-SW ; the northwestern and southeastern zones (1 and 0.5 km wide, respectively) are mainly occupied by ultramafic rocks, and the central zone (4 km wide) is composed of a layered gabbroic body,

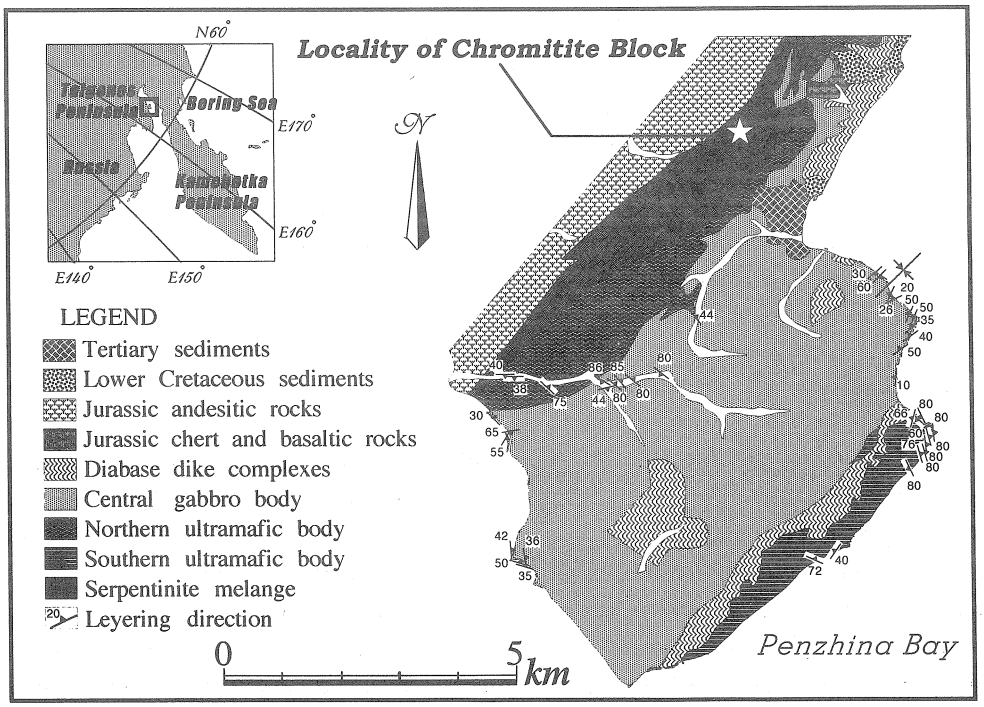

Fig. 1. Simplified geologic map of the Elistratova ophiolite by Saito et al. (in press).

which displays a gentle synclinal structure. An ophiolitic igneous complex composed of northern depleted mantle harzburgite (spinel Cr#= 40-75), ultramafic cumulates, noritic gabbro, and sheeted dikes of arc tholeiite affinity, as a whole, discordantly intruded into relatively fertile harzburgite (spinel Cr#= 30-55) on the south (Saito et al., in press). In northwestern margin of the ophiolite, serpentinite melange zone (1 km wide) develops along a fault between Jurassic andesitic volcanics and the ophiolite. The studied chromitite is found as a pebble size block (10×5 cm) in serpentinite melange zone (Fig. 1). Although Belyi and Akinin (1985) described some localities of podiform-type chromitite enclosed by dunite in both northern and southern peridotites, we could not find any chromitite from the intact peridotite bodies during our field research.

3. Petrography

The chromitite is composed of euhedral to subhedral chromian spinel (more than 95 vol.%) with serpentine and chlorite pseudomorphs after olivine and orthopyroxene. Primary olivine ($Fo_{91.0}$) is rarely preserved. Grain sizes of chromian spinel range from 0.5 to 2 mm. The chromian spinel grains rarely show the optical zoning, and they may be divided into two types, "core"-type and "ring"-type, based on the distribution of inclusions. Under the microscope, the core-type grain bears lighter-colored core containing many mineral inclusions and surrounded by inclusion-free rim (Fig. 2 a). The ring-type grain has inclusion-bearing light-colored ring between inclusion-free core and rim (Fig. 2 b). The compositional anomaly is more clearly seen in the back-scattered electron image (Fig. 3). The size of inclusion in rings (<10 μm) is smaller than that of cores (<20 μm mm). Inclusions are generally rounded in shape, and are generally distributed randomly in core or ring. Hornblende, Na-phlogopite, K-phlogopite and orthopyroxene are identified as inclusions. Although chlorite, talc, serpentine and hydrogarnet are also found as inclusions, they are considered as secondary phases which may have been altered from primary mafic minerals such as olivine and possibly plagioclase. Na-phlogopite forms polyphase inclusions with hornblende. Trails of fluid inclusions are sometimes observed in both inclusion-bearing and -free parts (Fig. 2 c). The fluid inclusions are commonly elongated (<5 μm) and often contain two phases, i.e. liquid and gas phases. Their fluid species are not yet determined.

4. Electron microprobe image of zoned chromian spinel and mineral chemistry

4.1 Analytical procedure

Chemical analyses of chromian spinel were carried out with a JEOL electron-probe microanalyzer JXA-8800R (WDS) at Center for Cooperative Research of Kanazawa University, and those of silicate inclusions were carried out with an AKASHI ALPHA-30 A scanning electron microscope equipped with a Philips EDAX-9100 energy-dispersive

analytical system (EDS) at Faculty of Science, Kanazawa University. The analyses were done at 15 kV accelerating voltage, 12 nA probe current on Faraday cup with probe current detector and 3 μm probe diameter for WDS, and at 20 kV accelerating voltage, 1 nA sample current on MgO and <2 μm beam diameter for EDS.

Cr, Si, Al and Fe X-ray mappings of two zoned chromian spinels were carried out with a JXA-8800R at 20 kV accelerating voltage, 50 nA probe current, 3×3 μm pixel size and 40 ms dwelling time.

4.2 Electron microprobe image and mineral chemistry

Electron microprobe images for Cr, Si, Al and Fe of two representative zoned chromian spinels are shown in Fig. 4. The inclusion-bearing part (optically light brownish color) contains significantly high Al and low Fe. The compositional change is consistent with distribution of inclusions. Representative analysis of the chromian spinel and the

	Core-type chromian spinel				*Ring-type chormian spinel*						*Olivine*		*Inclusions*			
	inclusion-bearing core		*inclusion-free rim*		*inclusion-free core*		*inclusion-bearing ring*		*inclusion-free rim*				*Hbl*	*Hbl*	*K-Phl*	*Na-Phl*
wt.%																
SiO_2	-	-	-	-	-	-	-	-	-	-	40.11	40.79	48.29	50.92	39.92	42.33
TiO_2	0.22	0.19	0.17	0.19	0.14	0.21	0.20	0.24	0.17	0.19	0.11	0.04	0.47	0.37	0.72	0.89
Al_2O_3	15.57	15.62	14.18	14.14	14.39	14.41	15.81	15.40	14.29	14.42	0.38	0.31	8.14	5.61	13.96	14.85
Cr_2O_3	54.60	54.51	53.13	54.74	54.69	54.45	54.38	54.71	54.23	53.98	0.45	0.45	3.53	3.00	4.12	3.63
Fe_2O_3	1.77	1.68	4.68	3.26	3.10	3.27	1.76	1.87	3.60	3.71						
FeO	14.76	14.74	14.84	14.76	14.93	14.65	14.48	14.80	14.68	14.66	8.79	8.74	2.07	1.80	4.63	1.12
MnO	0.45	0.44	0.58	0.50	0.46	0.57	0.46	0.50	0.53	0.57	0.20	0.21	0.04	0.06	0.08	0.09
MgO	12.73	12.70	12.33	12.51	12.45	12.58	12.91	12.69	12.52	12.54	49.69	49.92	21.46	22.04	24.95	26.02
CaO	-	-	-	-	-	-	-	-	-	-	0.01	0.03	10.72	11.51	0.04	0.09
Na_2O	-	-	-	-	-	-	-	-	-	-	-	-	2.65	1.73	0.18	6.54
K_2O	-	-	-	-	-	-	-	-	-	-	-	-	0.08	0.05	7.81	0.70
Total	100.10	99.88	99.90	100.10	100.15	100.14	99.99	100.20	100.02	100.06			97.45	97.09	96.41	96.26
atomic ratio																
O=	*4*	*4*	*4*	*4*	*4*	*4*	*4*	*4*	*4*	*4*	*4*	*4*	*23*	*23*	*22*	*22*
Si	-	-	-	-	-	-	-	-	-	-	0.983	0.991	6.784	7.127	5.600	5.705
Ti	0.005	0.005	0.004	0.005	0.003	0.005	0.005	0.006	0.004	0.005	0.002	0.001	0.050	0.039	0.076	0.090
Al	0.581	0.584	0.535	0.532	0.541	0.541	0.589	0.575	0.538	0.542	0.011	0.009	1.348	0.925	2.308	2.359
Cr	1.367	1.367	1.345	1.382	1.379	1.372	1.360	1.370	1.369	1.361	0.009	0.009	0.392	0.332	0.457	0.387
Fe^{3+}	0.042	0.040	0.113	0.078	0.074	0.078	0.042	0.044	0.086	0.089						
Fe^{2+}	0.391	0.391	0.397	0.394	0.398	0.390	0.383	0.392	0.392	0.391	0.180	0.178	0.243	0.211	0.543	0.126
Mn	0.012	0.012	0.016	0.013	0.012	0.015	0.012	0.013	0.014	0.015	0.004	0.004	0.005	0.007	0.010	0.010
Mg	0.601	0.601	0.589	0.595	0.592	0.598	0.608	0.599	0.596	0.596	1.815	1.808	4.494	4.598	5.218	5.228
Ca	-	-	-	-	-	-	-	-	-	-	0.000	0.001	1.614	1.726	0.006	0.013
Na	-	-	-	-	-	-	-	-	-	-	-	-	0.722	0.469	0.049	1.709
K	-	-	-	-	-	-	-	-	-	-	-	-	0.014	0.009	1.398	0.120
Total	3.000	3.000	2.999	2.999	3.000	2.999	3.000	3.000	2.999	2.999	3.005	3.000	15.665	15.444	15.665	15.747
Cr#	*0.702*	*0.701*	*0.715*	*0.722*	*0.718*	*0.717*	*0.698*	*0.704*	*0.718*	*0.715*						
Fe $^{3+}$ #	*0.021*	*0.020*	*0.057*	*0.039*	*0.037*	*0.039*	*0.021*	*0.022*	*0.043*	*0.045*						
Mg#	*0.606*	*0.606*	*0.597*	*0.602*	*0.598*	*0.605*	*0.614*	*0.604*	*0.603*	*0.604*	*0.910*	*0.911*	*0.949*	*0.956*	*0.906*	*0.976*

Table 1. Representative microprobe analysis of the rock-forming minerals. Fe_2O_3 and FeO of chromian spinel are recalculated by assuming spinel stoichiometry. Cr#, Fe^{3+}# and Mg# are $Cr/(Cr+Al)$, $Fe^{3+}/(Cr+Al+Fe^{3+})$ and $Mg/(Mg+Fe^{2+})$ atomic ratios, respectively.

inclusions are listed in Table 1. No chemical difference between core-type and ring-type is recognized.

The inclusion-bearing core and ring have almost constant $Mg/(Mg+Fe^{2+})$ ratio (0.

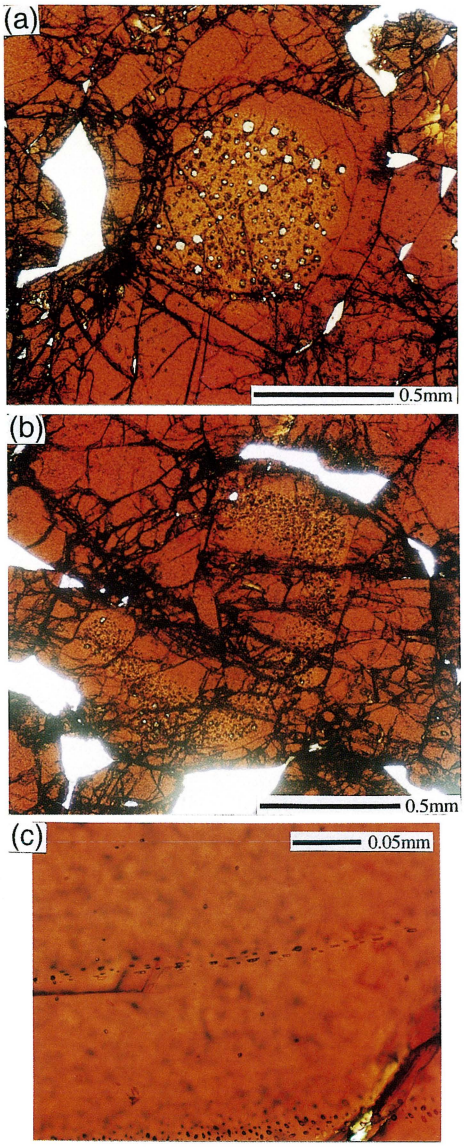

Fig. 2. Photomicrographs of zoned chromian spinel.
(a) Core-type.
(b) Ring-type.
(c) Fluid inclusions in chromian spinel.

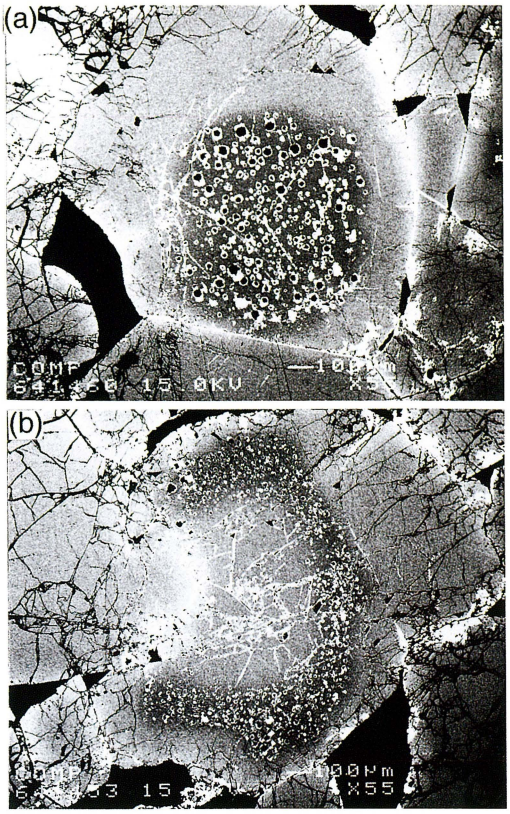

Fig. 3. Back-scattered electron image of the zoned chromian spinel.
(a) Core-type.
(b) Ring-type.

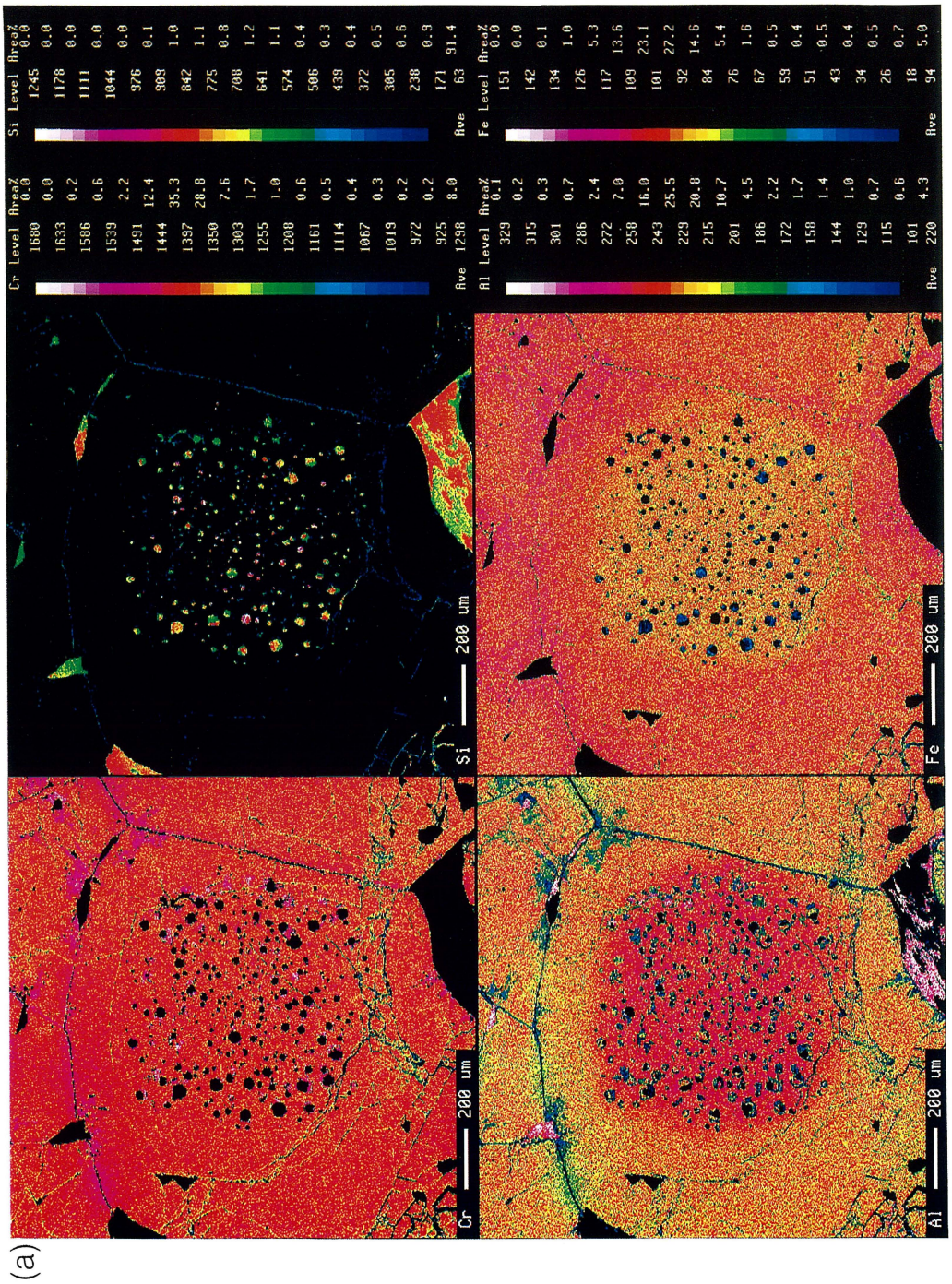

Fig. 4. Electron microprobe element image for Cr, Si, Al and Fe of zoned chromian spinel. (a) Core -type. (b) Ring-type.

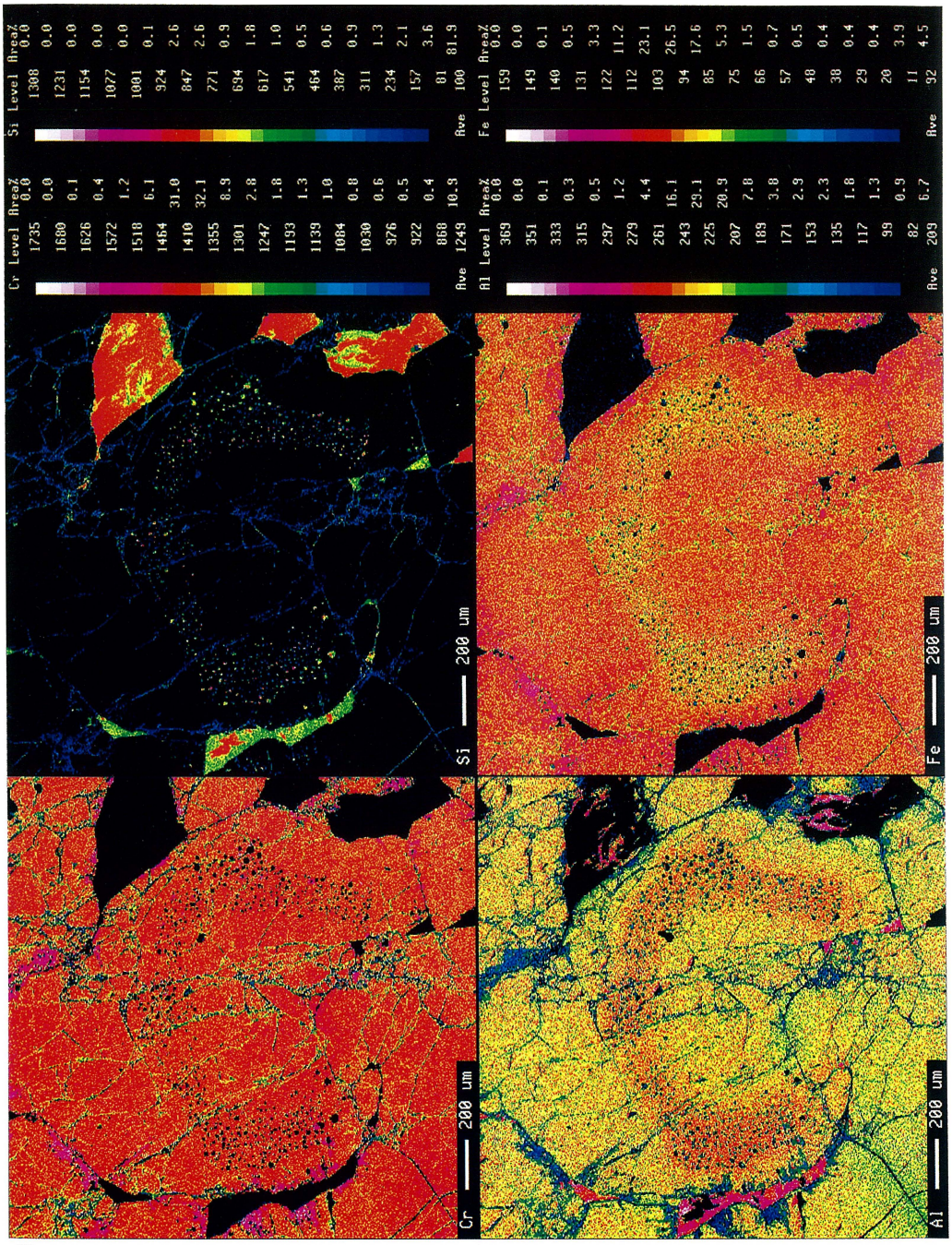
Cr Level Area%
1735 0.0
1680 0.0
1626 0.1
1572 0.4
1518 1.2
1464 6.1
1410 31.0
1355 32.1
1301 8.9
1247 2.8
1193 1.8
1139 1.3
1084 1.0
1030 0.8
976 0.6
922 0.5
868 0.4
Ave 1249 10.3
Si Level Area%
1308 0.0
1231 0.0
1154 0.1
1077 0.0
1001 0.0
924 0.1
847 2.6
771 2.6
694 0.9
617 1.8
541 1.0
464 0.5
387 0.6
311 0.9
234 1.3
157 2.1
81 3.6
Ave 100 81.9
Al Level Area%
369 0.0
351 0.0
333 0.1
315 0.3
297 0.5
279 1.2
261 4.4
243 16.1
225 29.1
207 20.9
189 7.8
171 3.8
153 2.3
135 1.8
117 1.3
99 0.9
82 6.7
Ave 209
Fe Level Area%
159 0.0
149 0.0
140 0.1
131 0.5
122 3.3
112 11.2
103 23.1
94 26.5
85 17.6
75 5.3
66 1.5
57 0.7
48 0.5
38 0.4
29 0.4
20 0.4
11 3.9
Ave 92 4.5
Cr 200 um
Si 200 um
Al 200 um
Fe 200 um

(b)

59-0.62). However, the inclusion-bearing part is characterized by lower $Fe^{3+}/(Cr+Al+Fe^{3+})$ ratio ($Fe^{3+}\#=0.011$-0.088) and $Cr/(Cr+Al)$ ratio ($Cr\#=0.69$-0.72) than those of inclusion-free part ($Fe^{3+}\#=0.033$-0.133; $Cr\#=0.71$-0.73) (Fig. 5 and Fig. 6 a). Ti content is relatively low in both inclusion-bearing and free parts (0.10-0.25 wt.%). The chemistry indicates that Al-Fe^{3+} substitution defines the compositional zoning rather than Al-Cr substitution. The Fe^{2+}-Mg partitioning constant ($K_D^{olivine-spinel}$) between olivine ($Fo_{91.0}$) and adjacent chromian spinel is 6.6-6.7, indicating relatively high equilibration temperature of about 850-900℃ by using Fabries (1979)'s thermometry.

Primary inclusions are characterized by high $Mg/(Mg+Fe^{2+})$ ratio ($Mg\#_{Na-phlogopite}=0.95$-$0.98$; $Mg\#_{hornblende}=0.95$; $Mg\#_{orthopyroxene}=0.94$; $Mg\#_{K-phlogopite}=0.91$). Hornblende has a composition with 1.5-2.7 wt.% Na_2O, 5.5-8.2 wt.% Al_2O_3, 0.23-0.60 wt.% TiO_2 and 6.

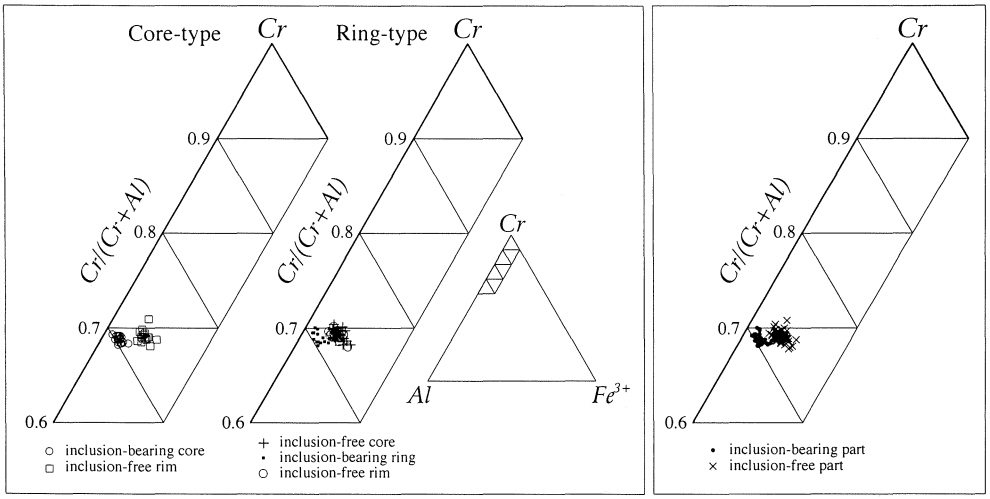

Fig. 5. Cr-Al-Fe^{3+} ternary diagram for zoned chromian spinel. All points in the left two diagrams are plotted together in the right diagram.

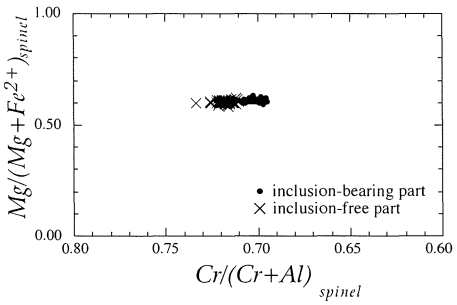

Fig. 6. Cr# versus Mg# diagram for zoned chromian spinel.

7-7.1 Si p.f.u.(O=23). Phlogopites contain 0.72-0.98 wt.% TiO_2, and the Na/(Na+K) ratio is 0.91-0.93 for Na-phlogopite and 0.03 for K-phlogopite.

5. Discussions

The current understanding of origin of podiform chromitite is that the podiform chromitite is a product of melt/mantle interaction and related melt mixing (e.g. Arai and Yurimoto, 1994 ; Zhou et al., 1994 ; Arai, 1997a ; Arai, 1997b). According to the model, chromian spinel is crystallized from a mixture consisting of successively supplied primitive magma and secondary SiO_2-rich melt, which had been produced by interaction between mantle harzburgite and supplied primitive magma. The hydrous mineral inclusions provide a critical evidence for crystallization of chromian spinel from fluid-bearing hydrous melt.

In the podiform chromitite, solid phase inclusions commonly occurs in chromian spinel, and diopside, enstatite, olivine, pargasitic amphibole, Na-phlogopite, K-phlogopite has been described as common silicate inclusions in chromian spinel of chromitite in the last decade (e.g. Talkington et al., 1986 ; Matsumoto et al., 1995 ; Melcher et al., 1997 ; Matsukage and Arai, 1998). Unusual inclusions such as jadeite, albite and nepheline were also found from chromitite pod in troctolite from Hess Deep (Matsukage and Arai, 1998). The hydrous mineral inclusions provide a critical evidence for crystallization of chromian spinel from fluid-bearing hydrous melt.

Chromian spinel in ophiolitic peridotite commonly shows Al-Cr zoning, either normal, reverse, or strongly asymmetric (Ishiwatari, 1985 ; Ozawa, 1986). Spinel phenocrysts in MORBs also show similar Al-Cr zoning, though spinel in oceanic island basalts and island arc basalts display Cr-(Al+Fe^{3+}) zoning (*ibid.*). These Cr-Al (Fe^{3+}) zoning of spinel may form through its incomplete reaction with fractionating magma. However, Al-Fe^{3+} zoning as observed in the Elistratova chromitite is extremely rare among natural Fe^{3+}-poor chromian spinels. Symmetric compositional zoning of chromian spinel may also form through subsolidus cation redistribution between spinel rim and adjacent mafic minerals after chromitite formation. In some metamorphosed peridotites, primary chromian spinel rimmed by ferrit-chromite, showing drastic change in Mg# and Fe^{3+}# in its margin, has been known (e.g. Arai, 1978 ; Kunugiza, 1981). In the Elistratova chromitite here studied, however, the compositional anomaly occurs only at inclusion-bearing core or ring, indicating the compositional change of the melt during spinel crystallization in the magma. As mentioned above, the hydrous inclusion-bearing core or ring is characterized by lower Fe^{3+}# than the inclusion-free part. The Fe^{3+}-Al zoning of the Elistratova chromitite indicates change in oxygen fugacity of melt during chromian spinel growth.

Recently, fluid inclusions containing high hydrogen (up to 69.5 mol.%) has been reported from chromian spinel in Kempirsai chromitite, Kazakhstan (Melcher et al., 1997). It is possible that hydrous melt to produce hydrous mineral inclusions contains some

reducing fluid species such as H_2 and CH_4 which reduce Fe^{3+} of chromian spinel. Such a process may most likely happen in the supra-subduction zone mantle, because various kinds of fluid may have been released from the subducted slab to the wedge mantle. This is compatible with our result that the Elistratova ophiolite may represent intrusion of the island-arc type magma into the shallow mantle in a supra-subduction zone setting (Saito et al., in press).

Acknowledgments

We express sincere thanks to Prof. S. Arai for his valuable advice on chromian spinel. We also thank Dr. O. Morozov, J. Hourigan, other supporting staffs and crew members of the ship for their help during our field survey. The senior author is grateful to T. Morishita for his discussion on zoned chromian spinel. Prof. K. Tazaki, Dr. Y. Tamura and H. Shukuno are also thanked for their help in electron microprobe analysis at Center for Cooperative Research of Kanazawa University. This study was supported in part by JSPS Research Fellowships for Young Scientists for the first author. Our field survey was supported by Science Technology Agency of Japan. Prof. S. Maruyama of Tokyo Institute of Technology in thanked for his help.

References

Arai, S. (1978) Contact metamorphosed dunite-harzburgite complex in the Chugoku District, Western Japan. *Contrib, Mineral. Petrol.*, **52**, 1-16.

Arai, S. (1997 a) Origin of podiform chromitites. *Jour. Asian Earth Sciences*, **15**, 303-310.

Arai, S. (1997 b) Control of wall-rock composition on the formation of podiform chromitites as a result of magma/peridotite interaction. *Resource Geol.*, **47**, 177-187.

Arai, S and Yurimoto, H. (1994) Podiform chromitites of the Tari-Misaka ultramafic complex, Southwest Japan, as mantle-melt interaction products. *Econ Geol.*, **89**, 1279-1288.

Belyi, V. F. and Akinin, V. V. (1985) Geologicheskoe Stroenie i Ofiolity Poluostrova Elistratova (Geological Structure and Ophiolites in Elistratova Peninsula). USSR Academy of Sciences, North-East Science Center (Magadan), 57 (Vol. 1) and 64 (Vol.2) pp. (in Russian)

Fabries, J. (1979) Spinel-olivine geothermometry in peridotites from ultramafic complexes. *Contrib. Mineral. Petrol.*, **69**, 329-336.

Ishiwatari, A. (1985) Igneous petrogenesis of the Yakuno ophiolite (Japan) in the context of the diversity of ophiolites. *Contrib. Mineral. Petrol.*, **89**, 155-167.

Ishiwatari, A., Miyashita, S., Saito, D., Tsujimori, T. (1998) Accretionary complexes and ophiolites in Taigonos Peninsula, far-eastern Russia. *Jour. Geol. Soc. Japan*, **104**, i - ii (color pages). (in Japanese)

Kunugiza, K. (1981) Tow contrasting types of zoned chromite of the Mt. Higashi-Akaishi peridotite body of the Sanbagawa metamorphic belt, central Shikoku. *Jour. Japan. Assoc. Min. Pet. Econ. Geol.*, **76**, 331-342.

Matsukage, K. and Arai, S. (1998) Jadeite, albite and nepheline as inclusions in spinel of chromitite from Hess Deep, equatorial Pacific: their genesis and implications for serpentinite diapir formation. *Contrib.*

Mineral. Petrol., **131**, 111-122.

Matsumoto, I., Arai, S. and Harada, T. (1995) Hydrous mineral inclusions in chromian spinel from the Yanomine ultramafic complexes of the Sangun zone, Southwest Japan. *Jour. Mineral. Petrol. Econ. Geol.*, **90**, 333-338. (in Japanese with English abstract)

Melcher, F., Grum, W., Simon, G., Thalhammer, T. V. and Stumpel, E. F. (1997) Petrogenesis of the ophiolitic giant chromite diopsits of Kempirsai, Kazakhstan: a study of solid and fluid inclusions in chromite. *Jour. Petrol.*, **38**, 1419-1458.

Ozawa, K. (1986) Partitioning of elements between constituents minerals in peridotites from the Miyamori ultramafic complex, Kitakami Mountains, Northeast Japan: Estimation of P-T condition and igneous composition of minerals. *Jour. Fac. Sci., Univ. Tokyo*, Sec. II, **21**, 115-137.

Saito, D., Ishiwatari, A., Tsujimori, T., Miyashita, S. and Sokolov, S. D. (in press) Elistratova ophiolite in Taiganos Peninsula, Far East Russia: An island arc ophiolite intruding into oceanic mantle. *Mem. Geol. Soc. Japan*. (in Japanese with English abstract)

Talkington, R. W., Watkinson, D. H., Whittaker, P. J. and Jones, P. C. (1986) Platinum group element-bearing minerals and other solid inclusions in chromite of mafic and ultramafic complexes : chemical compositions and comparisons. In : Carter, B. et al. (eds) Metallogeny of basic and ultrabasic rock (regional presentations). *Theophrastus Publications, Athens*, pp. 223-249.

Zhou, M. F., Robinson, P. T. and Bai, W.-J. (1994) Formation of podiform chromitites by melt/rock interaction in the upper mantle. *Mineral. Deposita*, **29**, 98-101.